Report

www.the-innovation.org

Mapping the emergence of visual consciousness in the human brain via brain-wide intracranial electrophysiology

Liang Shan,[1,2,6,*] Hui Huang,[3,6] Zhiting Zhang,[1,2] Yuyin Wang,[1,4] Fei Gu,[4,5] Mingwei Lu,[3] Wen Zhou,[4,5] Yi Jiang,[4,5,*] and Ji Dai[1,2,4,*]

*Correspondence: shanliang@siat.ac.cn (L.S.); yijiang@psych.ac.cn (Y.J.); ji.dai@siat.ac.cn (J.D.)

Received: January 28, 2022; Accepted: April 12, 2022; Published Online: April 20, 2022; https://doi.org/10.1016/j.xinn.2022.100243

GRAPHICAL ABSTRACT

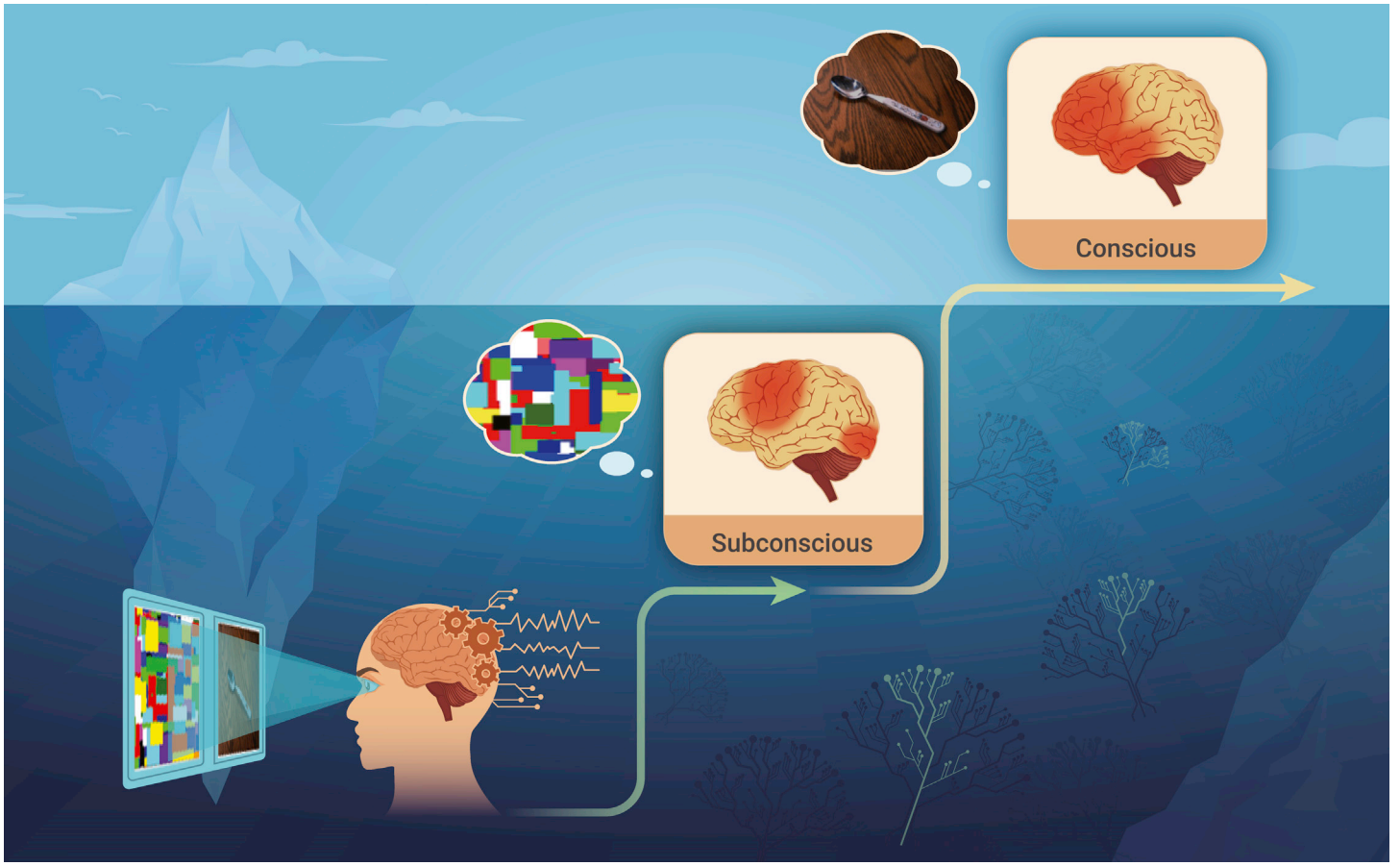

PUBLIC SUMMARY

- Understanding the biological basis of consciousness is an outstanding intellectual challenge
- The neural signatures underlying the emergence of visual consciousness were characterized
- A novel approach employing machine learning was used to analyze the massive iEEG data
- These findings extend the current understanding of the neural correlates of consciousness

Report

Mapping the emergence of visual consciousness in the human brain via brain-wide intracranial electrophysiology

Liang Shan,[1,2,6,*] Hui Huang,[3,6] Zhiting Zhang,[1,2] Yuyin Wang,[1,4] Fei Gu,[4,5] Mingwei Lu,[3] Wen Zhou,[4,5] Yi Jiang,[4,5,*] and Ji Dai[1,2,4,*]

[1]Guangdong Provincial Key Laboratory of Brain Connectome and Behavior, CAS Key Laboratory of Brain Connectome and Manipulation, The Brain Cognition and Brain Disease Institute (BCBDI), Shenzhen Institute of Advanced Technology, Chinese Academy of Sciences, Shenzhen 518055, China

[2]Shenzhen-Hong Kong Institute of Brain Science-Shenzhen Fundamental Research Institutions, Shenzhen 518055, China

[3]Department of Neurosurgery, The Second Affiliated Hospital of Nanchang University, Nanchang 330006, China

[4]University of Chinese Academy of Sciences, Beijing 100049, China

[5]State Key Laboratory of Brain and Cognitive Science, CAS Center for Excellence in Brain Science and Intelligence Technology, Institute of Psychology, Chinese Academy of Sciences, Beijing 100101, China

[6]These authors contributed equally

*Correspondence: shanliang@siat.ac.cn (L.S.); yijiang@psych.ac.cn (Y.J.); ji.dai@siat.ac.cn (J.D.)

Received: January 28, 2022; Accepted: April 12, 2022; Published Online: April 20, 2022; https://doi.org/10.1016/j.xinn.2022.100243

Citation: Shan L., Huang H., Zhang Z., et al., (2022). Mapping the emergence of visual consciousness in the human brain via brain-wide intracranial electrophysiology. The Innovation **3(3)**, 100243.

Consciousness lies at the heart of our existence and experience. To probe how perceptual consciousness emerges in the brain, we recorded brain-wide intracranial electroencephalography signals from human patients while their perceptual consciousness was effectively manipulated using the continuous flash suppression paradigm. We observed substantial differences in brain activities when visual information gradually enters consciousness. Specifically, the functional connectivity first increases and then decreases, oscillations in the low-frequency band reduce in power, and those in the high-frequency band remain unchanged. We employed random forest-based classification to characterize the transitions from no perception to subconsciousness and then to consciousness, which showed an increase in signal variance at the second transition rather than the first. Further, the frontal-parietal junction dominates the first transition, whereas the temporal-frontal lobes dominate the second transition. Finally, we identified the most relevant neuronal features associated with consciousness. Altogether, these findings shed fresh light on the emergence of visual consciousness.

INTRODUCTION

Understanding the biological basis of consciousness has been identified as an outstanding intellectual challenge across multiple disciplines including neuroscience, medicine, psychology, philosophy, and artificial intelligence.[1] Despite the distinct definitions of consciousness in different research fields, two mainstreams are evolving to tackle the neural correlates of consciousness. One direction is to find out the neural basis of a subject's overall conscious states such as being awake, coma, or vegetative. The other direction goes to understand how conscious percepts are generated, which is a major focus of cognitive neuroscience.[2] Even though our understanding of the nature of consciousness has been substantially improved in the past few decades, still many questions remain to be addressed. Among them, how perceptual consciousness emerges in the brain is arguably the most fundamental and intriguing one.

To unravel such a mystery, proper experimental paradigms and techniques are required. Previous studies have demonstrated that conscious perception can be effectively manipulated through a so-called continuous flash suppression (CFS)[3,4] paradigm. By presenting two different images to the two eyes and making one of the two competing stimuli dynamic and much stronger than the other, one can make the dynamic image dominant in perception and the other completely suppressed, thus generating the consciously invisible perception. The CFS paradigm together with the modified version—breaking-CFS (b-CFS)—offers a controllable and reliable means to manipulate visual consciousness, ranging from the subconscious to conscious perception, thus making it an ideal paradigm in studying consciousness.[5-7]

On the other hand, a variety of experimental techniques have been used to investigate the relationships between brain activity and the state of perceptual consciousness, most of which are noninvasive approaches including EEG, MEG, and fMRI in humans.[8-10] Given different techniques have different spatial and temporal resolutions, and the emergence of consciousness could transiently engage multiple cortical regions, the chance that these noninvasive approaches could precisely capture the emergence of consciousness would be low. Researchers also tried to get clues from single-unit, multi-unit, and local field potential recordings in monkeys,[11-13] yet it is almost impossible to simultaneously record from the whole brain in awake monkeys. Therefore, an invasive brain-wide recording technique with a high temporal and spatial resolution is needed. Intracranial electroencephalography (iEEG) using multiple electrodes placed inside the brain of patients with epilepsy offers a unique opportunity to record a large scale of signals simultaneously from a wide range of regions.[14-16] By combining recording sites from multiple subjects, it is possible to reconstitute a brain-wide mapping of the emergence of perceptual consciousness.

Such brain-wide recording raises a new challenge for data processing. The rise of machine learning meets the challenge as it can efficiently characterize the high dimensionality and multivariate nature of iEEG data in a way that is less affected by potential hypotheses.[17-19] In particular, the random forest (RF) classification, a bagging decision-tree-based model, is advantageous in decoding iEEG signals because of its less sensitivity to the multicollinearity and nonlinearity of electrophysiological data as well as its high interpretability.[20] The RF model has been widely applied in the pattern recognition of neural signals.[21,22]

In the current study, we aim to characterize the neural signatures of brain-wide electrophysiological signals during the emergence of perceptual consciousness by combining iEEG recording from human participants, the b-CFS paradigm, and a supervised machine learning algorithm (RF classification). Here we not only describe the brain-wide dynamics of electrophysiological activity and functional connectivity along with the transitions of the conscious states but also try to allocate the neural substrates responsible for the emergence of consciousness.

RESULTS

iEEG recording from humans with b-CFS paradigm

Seven participants (two females, mean age 24.0 ± 4.12) with electrodes implanted in the left hemisphere were involved in the current study. All subjects were instructed to perform a b-CFS task (Figure 1A), in which the suppressing stimuli (rapidly changing Mondrian patterns) were flashed on the left eye and the images to be perceived were presented on the right eye. During the experiment, the beginning period of each trial with no visual stimulus presented to the right eye served as the No Stimulus (NS) condition. Then a low-contrast image appeared as a subconscious stimulus (SubCon) with its contrast slowly increased. Participants were instructed to press a key immediately when they were aware of the image, and the image would dismiss instantly. Following a correct oral report of the perceived image, the test image was re-displayed in high contrast and acted as the conscious stimulus (Con). Luminance-balanced images of different categories (face/object/scene) and different valences (happy/neutral/fearful) were applied in the b-CFS task, and the data were pooled across different categories to tackle the emergence of perceptual consciousness in general.

Bipolar-referenced iEEG data were recorded from the implanted multi-lead electrodes while participants were performing the b-CFS task. Behavioral analysis indicated that the average reaction time (from image onset to keypress) of all participants was around 2.5–4.5 s (Figure 1B). To make use of most trials and avoid motor-related interference, signals from −2 to −0.5 s before the keypress were

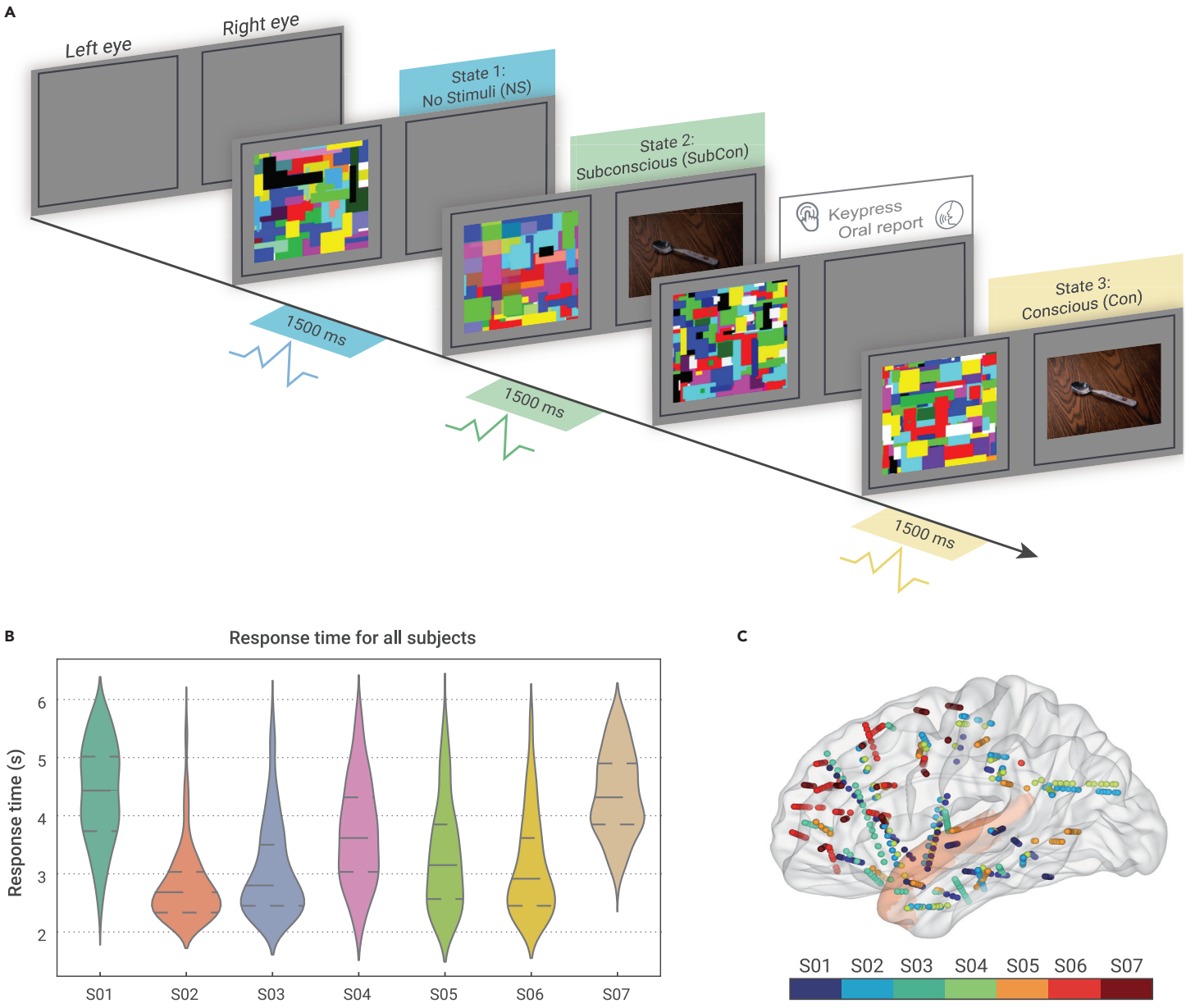

Figure 1. Experimental paradigm and iEEG recording (A) Illustration of the b-CFS paradigm. The suppressing stimuli (rapidly changing Mondrian patterns) were flashed to the left eye, and the images to be perceived were presented to the right eye. The No Stimulus (NS), Subconscious (SubCon), and Conscious (Con) states were indicated by blue, green, and yellow rectangles. The iEEG signals were extracted at epochs (1,500 ms long) corresponding to these three states. (B) Violin plots of the reaction time for all seven participants. Dashed lines indicated the mean and quartile. (C) Overview distribution of the recording sites for all seven participants in the left hemisphere. Orange shaded area indicates region STG. The color bar indicates different subjects.

extracted as 1.5-s-long iEEG segments to represent the subconscious state (SubCon). Accordingly, the same length of signals was extracted for the NS state and the Con state in each trial.

The location of each recording site was identified by co-registering post-implantation Computed Tomography (CT) to pre-implantation MRI scans with the guide of a high-resolution anatomical atlas (Brainnetome Atlas, see Supplemental materials).[23] After removing sites that located in white matter and sites that could not be registered to a brain region, a total of 662 recording sites covering most areas (20 out of 24 gyri; see detailed information in Table S1) of the left hemisphere were obtained. There were at least three recording sites from at least two participants in each brain region. An overview distribution of the recording sites for all seven participants is shown in Figure 1C (also see Figure S1).

Characteristics of iEEG signals during the emergence of consciousness

All iEEG signals were then run through pre-processing including band-pass filter (1–150 Hz), notch filter (50/100/150 Hz), and downsample (500 Hz) using EEGLAB toolkit.[24] Time-frequency representations (TFRs) of power were computed for every 1.5-s iEEG epoch of NS, SubCon, and Con states for each recording site. The raw outputs from the same brain region were averaged across recording sites and baseline corrected against the NS distributions at the individual level. Baseline-corrected TFRs of three states from the same brain region were averaged across participants to assess the neural dynamics during the emergence of consciousness. As an example, the averaged TFRs of region STG (superior temporal gyrus, orange shaded area in Figure 1C, see Table S1 for the full name list of brain regions) are shown in Figure 2A (see Figure S2 for the TFRs of the other 19 regions).

We noticed that in many brain regions there was a general trend of decrease in low-frequency power (e.g., theta, alpha) associated with the emergence of consciousness. To quantify such dynamics, we examined how the power spectral density (PSD) of the iEEG signals varied across NS, SubCon, and Con states. Figure 2B shows the values of PSD of all the 20 brain regions in the three states for each frequency band (theta: 4–8 hz; alpha: 8–13 hz; beta: 13–30 hz; low-gamma: 30–60 hz; medium-gamma: 60–100 hz; high-gamma: 100–150 Hz). The results showed that while the PSD of gamma band signals remained mostly constant, the PSD of theta, alpha, and beta bands decreased from NS to Con states (Figure 2B). A non-parametric test (Friedman test) was applied to assess the PSD

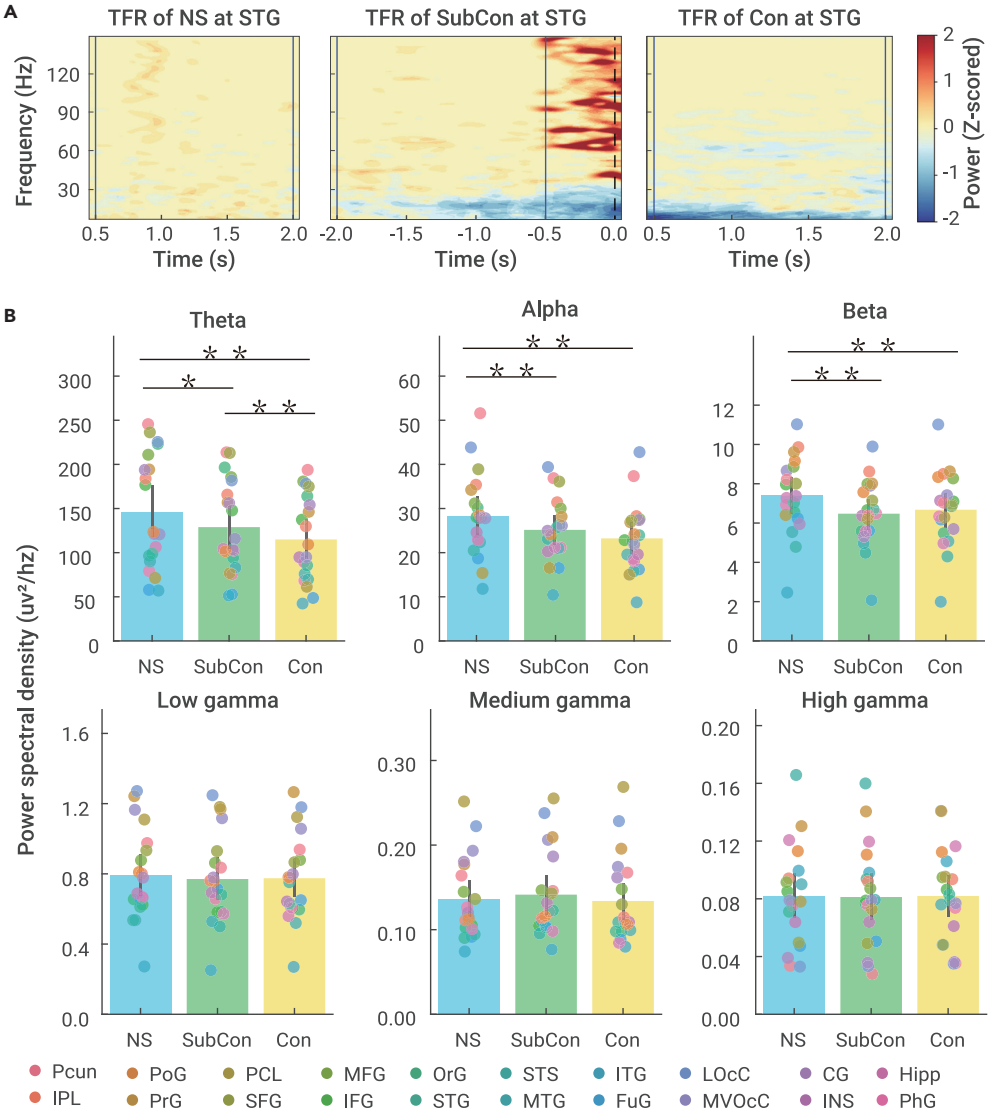

Figure 2. iEEG signal dynamics during the emergence of consciousness in the time-frequency domain (A) The averaged time-frequency representations of region STG (orange shaded area in Figure 1C) for the NS, SubCon, and Con states. Vertical blue lines indicate the segment period for each state. The dashed line indicates keypress. (B) The PSD from 20 brain regions in the NS, SubCon, and Con states for each frequency band. Error bar indicates SE. *p < 0.05; **p < 0.01.

differences between different conscious states for each frequency band and found significant differences in theta ($p < 0.001$), alpha ($p < 0.001$), and beta ($p < 0.001$) bands. Post-hoc analysis using Nemenyi test confirmed the significant differences between these pairs in theta band (NS versus SubCon: $p = 0.02$; SubCon versus Con: $p = 0.004$; NS versus Con: $p = 0.001$, multiple comparison with Bonferroni correction), alpha band (NS versus SubCon: $p = 0.004$; NS versus Con: $p = 0.001$), and beta band (NS versus SubCon: $p = 0.001$; NS versus Con: $p = 0.001$). Such dynamic PSD patterns of iEEG signals can serve as markers to identify the conscious level.

Dynamics of brain-wide functional connectivity

To reveal the brain-wide modulations in different conscious states, we constructed the functional connectivity (FC) maps for each consciousness state using the phase-locking value (PLV), which was used to assess whether there was a consistent phase difference between a pair of regions.[25,26] We computed the PLV of each pair for all 20 regions during the NS, SubCon, and Con states and show them in the circular graphs (Figures 3A–3C, see Table S1 for the full name list of brain region), which are organized according to the cortical lobes and separated by color as indicated in the flange (green for parietal lobe; yellow for frontal lobe; purple for temporal lobe; dark blue for occipital lobe; light blue for the limbic system). The results indicated a brain-wide increase of FC in the SubCon state (Figure 3B), then a systematic decrease in the Con state (Figure 3C, also see Figure 3F). We then constructed two adjacency matrices to represent the differences of FC between different conscious states in Figures 3D and 3E. An overall increase of FC (warm color representing positive value) could be observed during the transition from NS to SubCon state (Figure 3D) and an overall decrease (cold color representing negative value) could be seen during the transition from SubCon to Con state (Figure 3E). In particular, some regions of the temporal lobe (e.g., STS) showed large fluctuations during the emergence of consciousness compared with other parts (also see Figure S3 for the cortical lobe-based adjacency matrices). The mean PLVs for all frequency bands also showed a similar changing pattern in NS, SubCon, and Con states (Figure 3F). We used linear mixed-effects models with two phase- and six subband-fixed effects, and seven participant-random effects to assess the differences between conscious states and found significant differences between each pair (NS versus SubCon: $p = 0.002$; SubCon versus Con: $p = 0.000$; NS versus Con: $p = 0.032$, Bonferroni corrected). In brief, our results revealed that the brain-wide FC increased during the subconscious state but then decreased after consciousness was achieved.

Random forest classification of iEEG signals for different conscious states

To further delineate the differences between different conscious states, an RF classification-based machine learning approach[27] was applied to characterize the high dimensionality and multivariate iEEG signals. Figure 4A shows the pipeline of such a data-driven approach. Firstly, each of the 1.5-s pre-processed iEEG signals was re-segmented into three 0.5-s non-overlapping epochs. All EEG epochs were decomposed into six frequency bands including theta (4–8 Hz), alpha (8–13 Hz), beta (13–30 Hz), low-gamma (30–60 Hz), medium-gamma (60–100 Hz), and high-gamma (100–150 Hz). Seven Features from time-, frequency-, and nonlinear dynamical-domains were extracted for each frequency band, yielding a total of 42 features for each iEEG epoch. For each recording site, two RF classifiers were trained to classify iEEG signals of the three conscious states, aiming to capture the difference during the transitions from NS to SubCon state (transition 1: NS versus SubCon) and from SubCon to Con state (transition 2: SubCon versus Con). The classification ability of iEEG signals at each recording site was measured via the area under the receiver operating characteristic curve (AUC).[28-30] A higher AUC indicates better performance in discriminating different conscious states. A permutation-based statistic was used to determine the significance of the AUC in each transition for all recording sites by randomly permuting the phase labels and repeating the procedure 500 times, which produced a null AUC distribution that was used to obtain a p value for each actual AUC. We found that the AUCs calculated from all 662 recording sites in both transitions (NS versus SubCon and SubCon versus Con) were significantly greater than that for the null distribution ($p < 0.05$, permutation-based statistics with Bonferroni correction). As shown in Figure 4B, the AUCs for transitions 1 (NS versus SubCon, royal blue) and 2 (SubCon versus Con, coral) were distributed largely to the right of random level (red dash line at 0.5), especially that the second transition yielded higher AUCs. The mean AUCs across all recording sites for each participant are shown in the inset of Figure 4B, which indicated significant higher AUCs for transition 2 (SubCon

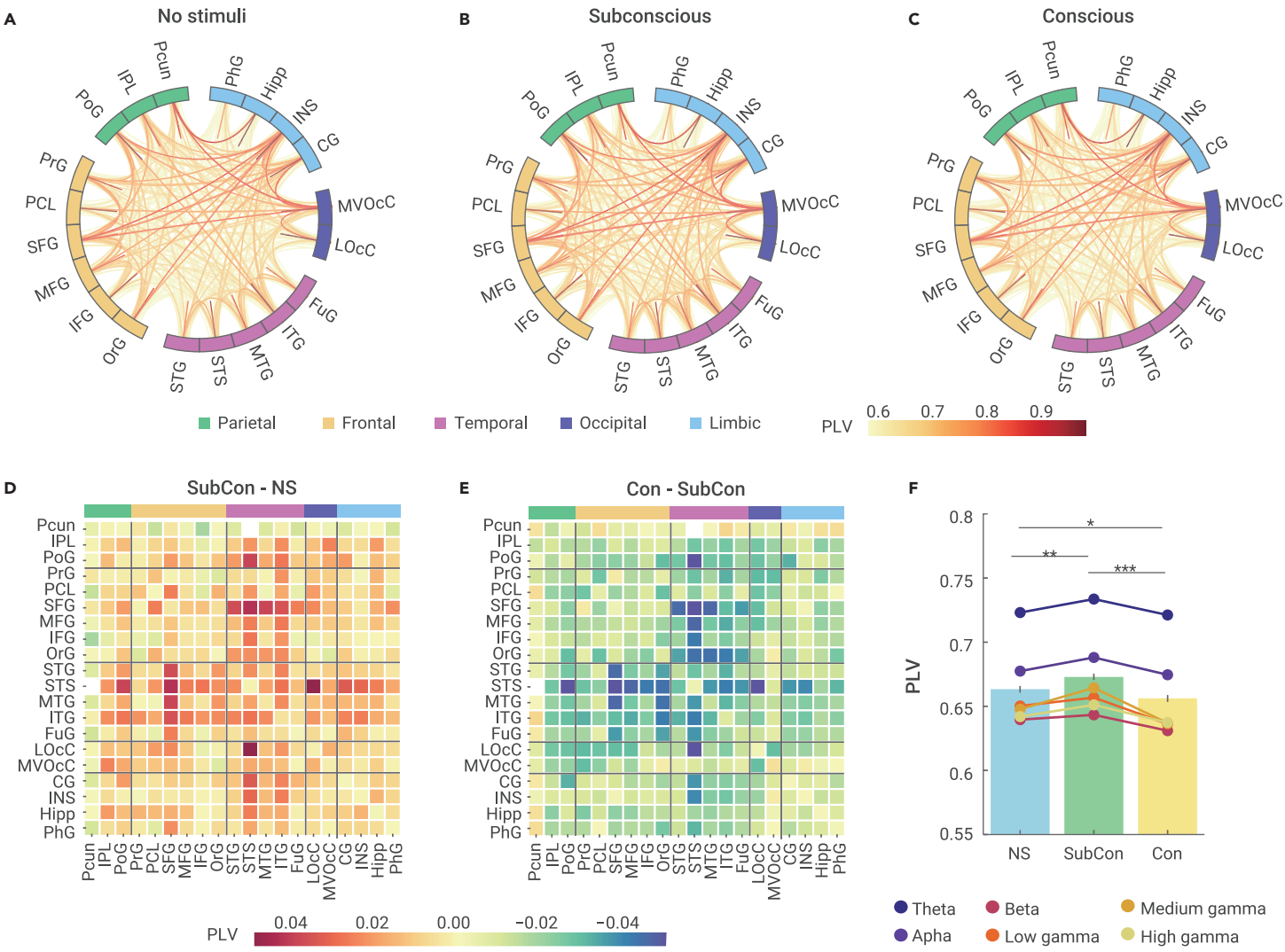

Figure 3. The dynamics of brain-wide functional connectivity (A–C) The phase-locking value (PLV) of each pair for all 20 regions during the NS (A), SubCon (B), and Con (C) states. The colors in the flange represent different cortical lobes. (D and E) The adjacency matrix for 20 regions represents the differences in FC between SubCon and NS (D), and Con and SubCon (E). The color bar indicates the PLV value. The solid lines divide different cortical lobes. (F) The mean PLVs for each frequency band in the NS, SubCon, and Con states. * indicates Bonferroni-corrected $p < 0.05$, **$p < 0.01$, and ***$p < 0.001$.

versus Con) than for 1 (NS versus SubCon), suggesting a higher discriminative capability for iEEG signals in the conscious state ($p = 0.033$, paired *t* test).

To further clarify the iEEG signal dynamics across different brain regions, the AUCs for all recording sites were plotted in Figure 4C, and the corresponding brain regions were coded by color. The x axis and y axis indicated transition 1 (NS versus SubCon) and transition 2 (SubCon versus Con), respectively. Consistent with Figure 4B, more points fell above the diagonal, indicating more sites had higher AUCs for transition 2. We then averaged the AUCs within the same regions and plotted them in Figure 4D, which also showed a significantly higher mean for transition 2 ($p = 0.001$, paired *t* test). As higher AUCs indicated stronger variation in neural activity, our results suggested that the variation of neural activity during consciousness was stronger than that during subconsciousness.

Region contribution to the emergence of consciousness

To clarify the contribution of different brain regions to different transitions during consciousness emergence, we then looked into the variation of regional AUCs for transitions 1 (NS versus SubCon) and 2 (SubCon versus Con). The regional AUC for each participant was calculated by averaging the data from all recording sites in the given region. To minimize the difference across individuals, the AUCs were *Z* scored before averaging across participants; then the mean regional AUCs were obtained for the 20 regions and displayed in the polar coordinate (Figure 5A for NS versus SubCon and Figure 5B for SubCon versus Con). We found that, during transition 1, regions around the junction of the parietal/frontal lobe (e.g., PrG) and the temporal/occipital lobe (e.g., LOcC) showed greater AUCs. However, during transition 2, the AUCs increased in most of the frontal and temporal lobes (e.g., OrG, STS). The differences in AUCs between these two transitions are shown in Figure 5C, which again pointed out the prominence of some regions in the temporal lobe (e.g., STS). Figures 5D–5I further show the *Z* scored AUCs and AUC differences for all recording sites in these two transitions (Figures 5D–5F, inner view; Figures 5D–5I, side view; see Videos S1–S3 for 3D animation), of which one dot indicated one recording site and darker red and larger size indicated greater AUCs. The linear mixed-effect models with classification-fixed effects and participants-random effects confirmed the significant differences between these two states in nine regions, which are shown in Cohen's d-based rendered images in Figures 5J and 5K and marked with asterisks in Figure 5C (see detailed statistics results in Table S1). It is worth noting that, although the distribution of these nine regions included the temporal lobe, parietal lobe, and limbic system, they established a cluster structure that was centered at STG/STS, suggesting that the STG/STS-centered regions played an essential role during the transition from subconsciousness to consciousness.

Feature importance that underpins consciousness

Finally, to uncover the influencing factors and the driving mechanism underlying the neural processing of consciousness emergence, the feature importance[31] was extracted from the RF framework, which quantified the contribution of each iEEG feature to the classification performance, allowing us to identify the most relevant neuronal features associated with consciousness emergence. Figure 6A showed the values of feature importance in the two transitions for all 42 features

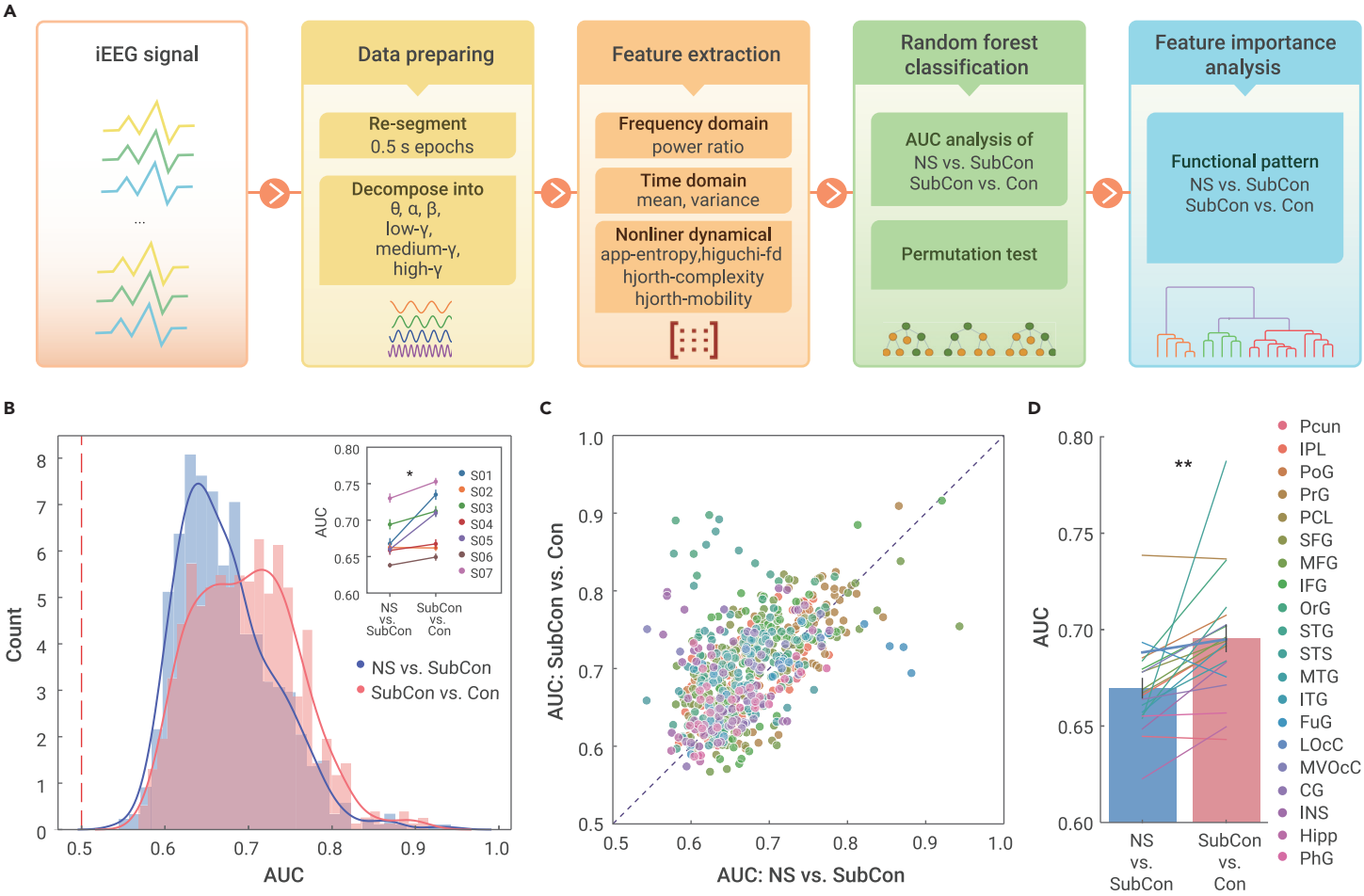

Figure 4. The data-driven machine learning approach and the classification ability of iEEG signals (A) The pipeline of the data-driven machine learning approach based on the random forest (RF) framework. (B) The distributions of AUCs for all 662 recording sites from transition 1 (NS versus SubCon, royal blue) and transition 2 (SubCon versus Con, coral). The red dashed line at 0.5 indicates the null distribution. The inset shows the mean AUCs for two transitions across all recording sites for each participant. (C) The scatterplot of AUCs for all recording sites. The x axis and y axis indicate the AUCs for NS versus SubCon, and SubCon versus Con, respectively. Sites from different regions are color-coded as indicated in (D). (D) The averaged AUCs within the same regions for NS versus SubCon and SubCon versus Con. The regions are color-coded and shown on the right. The royal blue and coral columns indicate the mean AUCs for all regions with the error bar indicating SE.

(six frequency bands × seven feature types, royal blue for NS versus SubCon, coral for SubCon versus Con). In general, we found that power ratio (i.e., the relative spectral power) and variance (i.e., squared deviation) were the two most important features across all six frequency bands and two transitions.

Then we examine the dynamics of the feature importance for the power ratio and the variance across different brain regions. The regional feature importance values were obtained by averaging within the same regions, which are shown in Figures 6B and 6C and organized according to the cortical lobes. Although the feature importance of the power ratio and the variance showed complex patterns across regions, there are some characteristics worth noticing. For example, the contribution of the power ratio to RF classifications mainly came from the frontal lobe in the gamma band, of which several regions (SFG, MFG, IFG, and OrG) showed similar patterns in both transitions (Figure 6B). The power ratio from two regions of the temporal lobe (STG, STS) also contributed a lot during transition 2 (Figure 6B). On the contrary, the variance of the medium-gamma band from multiple regions in the temporal lobe (ITG, FuG), occipital lobe (MVOcC), and limbic system (Amyg, PhG) contributed a lot to both transitions (Figure 6C).

As the diversity of feature importance implied functional differentiation among regions during the emergence of consciousness, we next sought to uncover the hidden functional structure of these regions by taking advantage of the similarity of feature importance. We used a hierarchical clustering algorithm, which belongs to the data-driven unsupervised machine learning approach,[32] to cluster these 20 regions by their feature importance values. We found these regions were automatically clustered into three groups in both transitions (Figure 6D for NS versus SubCon and Figure 6E for SubCon versus Con). It is worth noting that regions from the frontal lobe (OrG, PrG, SFG, MFG, IFG, but not PCL) were always clustered into one independent group in both transitions (orange in Figures 6D and 6E), suggesting that these regions were functionally close in the stage of consciousness emergence. In addition, although PCL was traditionally classified to the frontal lobe in the standard brain atlas, the cluster results indicated that its functional pattern was different from other regions in the frontal lobe but was similar to regions in the parietal/occipital lobe (Figures 6D and 6E), suggesting that PCL should be considered as a parietal region.

DISCUSSION

In this study, we combined the large-scale iEEG and the machine learning-based analysis to unravel the neural substrates and the functional dynamics of consciousness emergence in the human brain. Our results provided a comprehensive characterization of the activity of most brain regions during the emergence of visual consciousness in the human brain. We showed the dynamics of the FC and the oscillations in signal power during the transitions from no perception to subconsciousness and then to consciousness, and we further showed the functional dominance of the frontal-parietal junction in the first transition and the temporal-frontal lobes in the second transitions. Given these results were obtained in an unbiased data-driven approach, we believe these findings substantially add to and extend our understanding of the neural correlates of consciousness emergence.

The neural correlates of consciousness emergence

One of the fundamental questions in understanding consciousness is to clarify the neural correlates of consciousness.[2,33,34] Consistent with the Global Neuronal Workspace Theory (GNWT),[35] we found that a broad range of cortical regions was involved in the generation of perceptual consciousness rather than a localized nucleus serving as the hub. During such a process, the brain-wide FC was

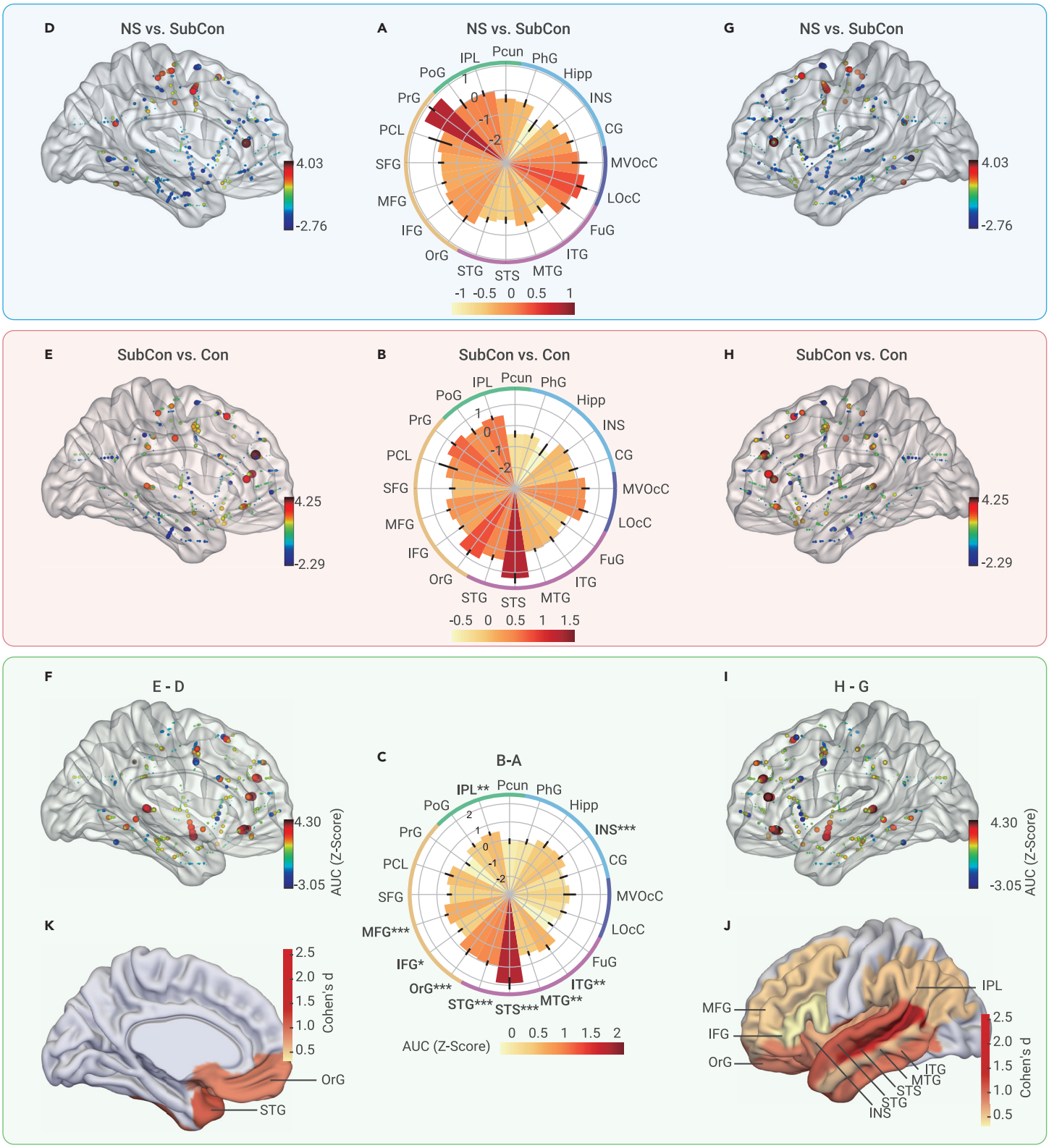

Figure 5. Regional contribution to the emergence of consciousness (A and B) The polar plots of the *Z* scored AUCs for the 20 regions for NS versus SubCon (A) and SubCon versus Con (B). The colors in the flange indicate different cortical lobes as in Figure 3A. (C) The differences in the *Z* scored AUCs between the two transitions in (A) and (B) . Asterisks indicate significant differences. The error bar indicates SE (see Table S1 for more statistical details). (D–I) *Z* scored AUCs and AUC differences for all recording sites in the two transitions. (D–F) inner view; (G–I) side view. The AUC of each site is coded by both color and size. The color bar indicates *Z* scored AUC. (J and K) The rendered images are based on Cohen's d denoting the differences between transitions 1 and 2. (J) side view; (K) inner view.

enhanced in the subconscious state and then faded in the conscious state, indicating that stronger synchronization is required for the brain to achieve perceptual consciousness. Once the consciousness is achieved, the synchronization returns to a lower level. Such synchronization is a temporary state that dismisses soon after the consciousness is achieved and maintained. Regardless of the FC dynamics, it is not yet clear whether a synchronization threshold is required for the whole brain or within a portion of the brain to achieve consciousness. Of interest, the temporal lobe showed larger FC fluctuation than the frontal lobe (Figure S3), suggesting that the functions of these temporal regions in the emergence of consciousness have been largely underestimated by previous studies.

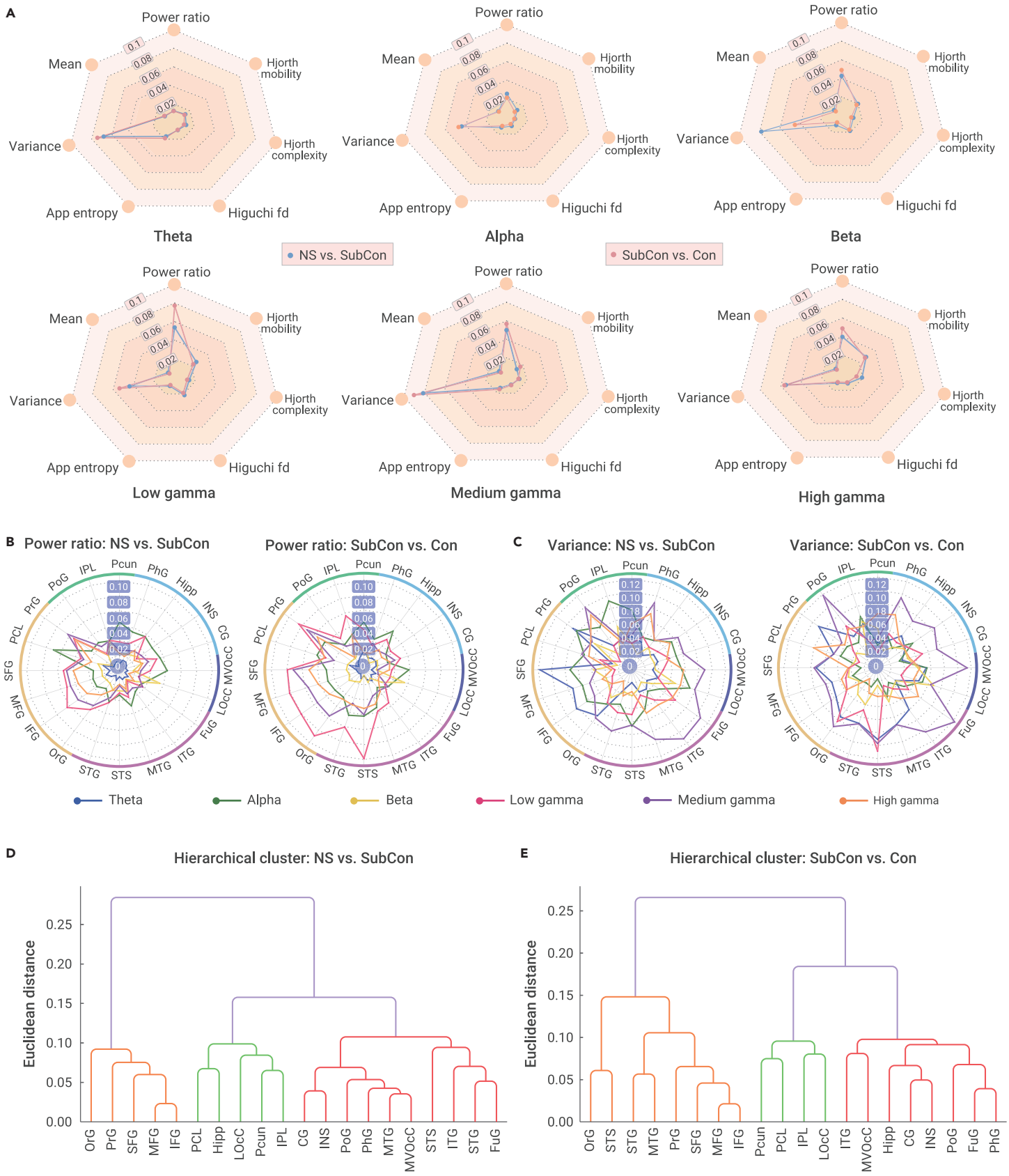

Figure 6. Feature extraction and the regional contribution of feature importance (A) The values of feature importance were extracted for all 42 features (six frequency bands × seven feature types) from the fitted RF models in the two transitions. Royal blue represents NS versus SubCon; coral represents SubCon versus Con. (B) The averaged values of feature importance for feature "Power Ratio" were plotted against the recording regions in polar coordinates for NS versus SubCon (left) and SubCon versus Con (right). The colors of the central curves represent different frequency bands as indicated on the bottom. The colors in the flange indicate different cortical lobes as in Figure 3. (C) The averaged values of feature importance for feature "Variance" were plotted against the recording regions in polar coordinates. The definitions are the same as in (B). (D and E) The results of the hierarchical cluster for the 20 regions were based on feature importance values. (D) NS versus SubCon; (E) SubCon versus Con.

Consistently, the RF classification revealed that while the frontal and the occipital lobes showed higher ability in classifying the NS versus SubCon states, the temporal lobe showed the highest ability in classifying the SubCon versus Con states (Figure 5). Altogether, our study points out the significance of the STG/STS-centered regions in the emergence of consciousness.

The temporal lobe has been studied using a similar CFS paradigm while recording electrocorticographic (ECoG) signals, which also supported that STS is responsible for conscious perception.[6] However, ECoG can only record surface signals from a limited area. Our study employed depth electrodes and recorded signals from the brain-wide scale, thus providing additional information regarding the functions of other areas. For example, we found that the occipital lobe was more dominant during transition 1 than in transition 2 (Figures 5A and 5B), which seems in line with that the primary visual area (V1) is important for nonconscious perception but not essential for conscious perception. A controversial theory proposed that the dorsal and ventral visual streams are associated with nonconscious and conscious perception, respectively.[36] Our result does support that the frontal-parietal junction plays an important role in subconscious processing and that the temporal lobe dominates conscious perception. On the other hand, the finding that the frontal lobe is also essential for conscious perception lends support to the notion that the subconscious and the conscious processes may work as the two sides of the same coin to guide human behaviors.

Overall, regarding the two popular theories of consciousness, our results seem to be more in line with the GNWT rather than Integrated Information Theory (IIT),[37] as we did find increased activation in frontal-parietal areas as predicted by GNWT yet did not find sustained activity in the posterior zones that are predicted by the IIT.[38]

The physiological markers for consciousness

Being able to monitor the conscious state of humans would be particularly useful for clinical diagnosis and treatment. Therefore, identifying reliable physiological markers of the conscious states turns out to be essential. Previously some studies suggested that long-distance gamma synchrony may correlate with visual consciousness,[39,40] yet later studies indicated that gamma band oscillations were not necessary for visual perception as gamma synchrony can be present in the subconsciousness state.[41,42] In our study, we found the power of iEEG signals in the time-frequency domain could serve as physiological markers as they showed unique changing patterns across different conscious states. Specifically, as the consciousness of visual stimulation emerged, the power of the theta/alpha/beta bands decreased, while the gamma band remained almost constant. Notably, the power increase around 60 Hz could be seen in multiple regions including Pcun, PoG, PrG, PCL, and MFG during the subconscious state (Figure S2). It is not yet clear whether such a frequency band has any special role in consciousness emergence. Overall, the changing trend of the power in the low- and high-frequency band was even obvious for regions in the frontal, parietal, and occipital lobes (e.g., PrG, PCL) (Figure S2). Given the neural activity in these lobes can also be captured by EEG recording, it is possible to use EEG signals as the data source and develop noninvasive devices to monitor the conscious state.

MATERIALS AND METHODS

Detailed description of the materials and methods can be found online at https://doi.org/10.1016/j.xinn.2022.100243.

REFERENCES

1. Miller, G. (2005). What is the biological basis of consciousness? Science ***309***, 79.
2. Rees, G., Kreiman, G., and Koch, C. (2002). Neural correlates of consciousness in humans. Nat. Rev. Neurosci. ***3***, 261–270.
3. Pournaghdali, A., and Schwartz, B.L. (2020). Continuous flash suppression: known and unknowns. Psychon. Bull. Rev. ***27***, 1071–1103.
4. Fang, F., and He, S. (2005). Cortical responses to invisible objects in the human dorsal and ventral pathways. Nat. Neurosci. ***8***, 1380–1385.
5. Jiang, Y., and He, S. (2006). Cortical responses to invisible faces: dissociating subsystems for facial-information processing. Curr. Biol. ***16***, 2023–2029.
6. Baroni, F., van Kempen, J., Kawasaki, H., et al. (2017). Intracranial markers of conscious face perception in humans. NeuroImage ***162***, 322–343.
7. Stein, T., Hebart, M.N., and Sterzer, P. (2011). Breaking continuous flash suppression: a new measure of unconscious processing during interocular suppression? Front. Hum. Neurosci. ***5***, 167.
8. Grill-Spector, K., Kushnir, T., Hendler, T., and Malach, R. (2000). The dynamics of object-selective activation correlate with recognition performance in humans. Nat. Neurosci. ***3***, 837–843.
9. Schurger, A., Sarigiannidis, I., Naccache, L., et al. (2015). Cortical activity is more stable when sensory stimuli are consciously perceived. Proc. Natl. Acad. Sci. U S A ***112***, E2083–E2092.
10. Fan, L. (2021). Mapping the human brain: what Is the next Frontier? Innovation ***2***, 100073.
11. Leopold, D.A., and Logothetis, N.K. (1996). Activity changes in early visual cortex reflect monkeys' percepts during binocular rivalry. Nature ***379***, 549–553.
12. Maier, A., Logothetis, N.K., and Leopold, D.A. (2007). Context-dependent perceptual modulation of single neurons in primate visual cortex. Proc. Natl. Acad. Sci. U S A ***104***, 5620–5625.
13. Wilke, M., Mueller, K.M., and Leopold, D.A. (2009). Neural activity in the visual thalamus reflects perceptual suppression. Proc. Natl. Acad. Sci. U S A ***106***, 9465–9470.
14. Lachaux, J.P., Rudrauf, D., and Kahane, P. (2003). Intracranial EEG and human brain mapping. J. Physiol. Paris ***97***, 613–628.
15. Wang, Y., Yan, J., Wen, J., et al. (2016). An intracranial electroencephalography (iEEG) brain function mapping tool with an application to epilepsy surgery evaluation. Front. Neuroinf. ***10***, 15.
16. Parvizi, J., and Kastner, S. (2018). Promises and limitations of human intracranial electroencephalography. Nat. Neurosci. ***21***, 474–483.
17. Thiery, T., Saive, A.-L., Combrisson, E., et al. (2020). Decoding the neural dynamics of free choice in humans. PLoS Biol. ***18***, e3000864.
18. Zhang, J., Yin, Z., Chen, P., and Nichele, S. (2020). Emotion recognition using multi-modal data and machine learning techniques: a tutorial and review. Inf. Fusion ***59***, 103–126.
19. Xu, Y., Liu, X., Cao, X., et al. (2021). Artificial intelligence: a powerful paradigm for scientific research. Innovation ***2***, 100179.
20. Iwama, S., Tsuchimoto, S., Hayashi, M., et al. (2020). Scalp electroencephalograms over ipsilateral sensorimotor cortex reflect contraction patterns of unilateral finger muscles. NeuroImage ***222***, 117249.
21. Feczko, E., Balba, N., Miranda-Dominguez, O., et al. (2018). Subtyping cognitive profiles in autism spectrum disorder using a functional random forest algorithm. Neuroimage ***172***, 674–688.
22. Engemann, D.A., Kozynets, O., Sabbagh, D., et al. (2020). Combining magnetoencephalography with magnetic resonance imaging enhances learning of surrogate-biomarkers. Elife ***9***, e54055.
23. Fan, L., Li, H., Zhuo, J., et al. (2016). The human brainnetome atlas: a new brain atlas based on connectional architecture. Cereb. Cortex ***26***, 3508–3526.
24. Delorme, A., and Makeig, S. (2004). EEGLAB: an open source toolbox for analysis of single-trial EEG dynamics including independent component analysis. J. Neurosci. Methods ***134***, 9–21.
25. Johnson, E.L., Adams, J.N., Solbakk, A.-K., et al. (2018). Dynamic frontotemporal systems process space and time in working memory. PLoS Biol. ***16***, e2004274.
26. Solomon, E.A., Stein, J.M., Das, S., et al. (2019). Dynamic theta networks in the human medial temporal lobe support episodic memory. Curr. Biol. ***29***, 1100–1111.e4.
27. Breiman, L. (2001). Random forests. Mach. Learn. ***45***, 5–32.
28. Gui, P., Jiang, Y., Zang, D., et al. (2020). Assessing the depth of language processing in patients with disorders of consciousness. Nat. Neurosci. ***23***, 761–770.
29. Hermann, B., Salah, A.B., Perlbarg, V., et al. (2020). Habituation of auditory startle reflex is a new sign of minimally conscious state. Brain ***143***, 2154–2172.
30. Ramaswamy, S.M., Kuizenga, M.H., Weerink, M.A., et al. (2019). Novel drug-independent sedation level estimation based on machine learning of quantitative frontal electroencephalogram features in healthy volunteers. Br. J. Anaesth. ***123***, 479–487.
31. Engemann, D.A., Raimondo, F., King, J.-R., et al. (2018). Robust EEG-based cross-site and cross-protocol classification of states of consciousness. Brain ***141***, 3179–3192.
32. Iddas, H., and Iramina, K. (2021). Directed EEG functional connectivity features to reveal different attention indexes using hierarchical clustering. IEEE Access ***9***, 59328–59335.
33. Calabro, R.S., Cacciola, A., Bramanti, P., and Milardi, D. (2015). Neural correlates of consciousness: what we know and what we have to learn! Neurol. Sci. ***36***, 505–513.
34. Koch, C., Massimini, M., Boly, M., and Tononi, G. (2016). Neural correlates of consciousness: progress and problems. Nat. Rev. Neurosci. ***17***, 307–321.
35. Mashour, G.A., Roelfsema, P., Changeux, J.P., and Dehaene, S. (2020). Conscious processing and the global neuronal Workspace hypothesis. Neuron ***105***, 776–798.
36. Milner, A.D., and Goodale, M.A. (2008). Two visual systems re-viewed. Neuropsychologia ***46***, 774–785.
37. Tononi, G., Boly, M., Massimini, M., and Koch, C. (2016). Integrated information theory: from consciousness to its physical substrate. Nat. Rev. Neurosci. ***17***, 450–461.
38. Melloni, L., Mudrik, L., Pitts, M., and Koch, C. (2021). Making the hard problem of consciousness easier. Science ***372***, 911–912.
39. Melloni, L., Molina, C., Pena, M., et al. (2007). Synchronization of neural activity across cortical areas correlates with conscious perception. J. Neurosci. ***27***, 2858–2865.
40. Rodriguez, E., George, N., Lachaux, J.P., et al. (1999). Perception's shadow: long-distance synchronization of human brain activity. Nature ***397***, 430–433.
41. Luo, Q., Mitchell, D., Cheng, X., et al. (2009). Visual awareness, emotion, and gamma band synchronization. Cereb. Cortex ***19***, 1896–1904.
42. Pockett, S., and Holmes, M.D. (2009). Intracranial EEG power spectra and phase synchrony during consciousness and unconsciousness. Conscious Cogn. ***18***, 1049–1055.

ACKNOWLEDGMENTS

This work was supported by the National Natural Science Foundation of China (U20A2017, 31830037), the Science and Technology Funds of Guangdong Province (2020A1515111118, 2022A1515010134), the Youth Innovation Promotion Association of Chinese Academy of Sciences (2017120), the Shenzhen-Hong Kong Institute of Brain Science–Shenzhen Fundamental Research Institutions (NYKFKT2019009), and the Strategic

Priority Research Program of Chinese Academy of Sciences (XDBS01030100, XDB32010300), the Ministry of Science and Technology of the People's Republic of China (2021ZD0203800), and the Fundamental Research Funds for the Central Universities.

AUTHOR CONTRIBUTIONS

L.S. and J.D. designed the experiment; H.H. and M.L. performed the surgery; L.S. and H.H collected the data; L.S., Z.Z, Y.W., and F.G. analyzed the data; L.S. and J.D prepared the figures; L.S., J.D., W.Z, and Y.J. wrote the manuscript.

DECLARATION OF INTERESTS

The authors declare no competing interests.

SUPPLEMENTAL INFORMATION

Supplemental information can be found online at https://doi.org/10.1016/j.xinn.2022.100243.

LEAD CONTACT WEBSITE

http://bcbdi.siat.ac.cn/index.php/member2/showMember/nid/25.shtml.